BASIC RESEARCH www.jasn.org

Klotho Prevents Renal Calcium Loss

R. Todd Alexander,*† Titia E. Woudenberg-Vrenken,* Jan Buurman,* Henry Dijkman,‡ Bram C. J. van der Eerden,§ Johannes P.T.M. van Leeuwen,§ René J. Bindels,* and Joost G. Hoenderop*

*Department of Physiology, Nijmegen Centre for Molecular Life Sciences, Nijmegen, The Netherlands; †Department of Pediatrics, University of Alberta, Alberta, Canada; ‡Department of Pathology, Radboud University Nijmegen Medical Centre, Nijmegen, The Netherlands; and §Department of Internal Medicine, Erasmus Medical Center, Rotterdam, The Netherlands

ABSTRACT

Disturbed calcium (Ca^{2+}) homeostasis, which is implicit to the aging phenotype of klotho-deficient mice, has been attributed to altered vitamin D metabolism, but alternative possibilities exist. We hypothesized that failed tubular Ca^{2+} absorption is primary, which causes increased urinary Ca^{2+} excretion, leading to elevated 1,25-dihydroxyvitamin D_3 [1,25$(OH)_2D_3$] and its sequelae. Here, we assessed intestinal Ca^{2+} absorption, bone densitometry, renal Ca^{2+} excretion, and renal morphology via energy-dispersive x-ray microanalysis in wild-type and klotho$^{-/-}$ mice. We observed elevated serum Ca^{2+} and fractional excretion of Ca^{2+} (FE_{Ca}) in klotho$^{-/-}$ mice. Klotho$^{-/-}$ mice also showed intestinal Ca^{2+} hyperabsorption, osteopenia, and renal precipitation of calcium-phosphate. Duodenal mRNA levels of transient receptor potential vanilloid 6 (TRPV6) and calbindin-D_{9K} increased. In the kidney, klotho$^{-/-}$ mice exhibited increased expression of TRPV5 and decreased expression of the sodium/calcium exchanger (NCX1) and calbindin-D_{28K}, implying a failure to absorb Ca^{2+} through the distal convoluted tubule/connecting tubule (DCT/CNT) via TRPV5. Gene and protein expression of the vitamin D receptor (VDR), 25-hydroxyvitamin D-1-α-hydroxylase (1αOHase), and calbindin-D_{9K} excluded renal vitamin D resistance. By modulating the diet, we showed that the renal Ca^{2+} wasting was not secondary to hypercalcemia and/or hypervitaminosis D. In summary, these findings illustrate a primary defect in tubular Ca^{2+} handling that contributes to the precipitation of calcium-phosphate in DCT/CNT. This highlights the importance of klotho to the prevention of renal Ca^{2+} loss, secondary hypervitaminosis D, osteopenia, and nephrocalcinosis.

J Am Soc Nephrol 20: 2371–2379, 2009. doi: 10.1681/ASN.2008121273

Characterization of a mouse that showed a phenotype comparable to human aging led to the identification of the hormone klotho.[1] Klotho$^{-/-}$ mice have atherosclerosis, osteopenia, soft tissue calcifications, pulmonary emphysema, and altered glucose metabolism.[1] It has been suggested that the etiology of many of these findings is a primary defect in phosphorous [P(i)] and calcium (Ca^{2+}) homeostasis.[2,3] Klotho$^{-/-}$ mice have elevated serum levels of Ca^{2+}.[1,4,5] The mechanism mediating hypercalcemia is poorly understood. A possible explanation invokes the role of klotho in vitamin D homeostasis. Klotho has been proposed to participate in a negative feedback circuit to inhibit 1,25-dihydroxyvitamin D_3 [1,25$(OH)_2D_3$] synthesis.[6,7] Specifically, klotho is necessary to transduce the signal

Received December 17, 2008. Accepted July 10, 2009.

Published online ahead of print. Publication date available at www.jasn.org.

R.T.A. and T.E.W.-V. contributed equally to this work.

Correspondence: Dr. Joost G. Hoenderop, 286 Physiology, Radboud University, Nijmegen Medical Centre, PO Box 9101, 6500 HB Nijmegen, The Netherlands. Phone: 31-24-3610580; Fax: 31-24-3616413; E-mail: J.Hoenderop@fysiol.umcn.nl

of fibroblast growth factor 23 (FGF23) through the FGF receptor, thereby suppressing CYP1b expression, the enzyme that mediates the conversion of 25-hydroxyvitamin D into $1,25(OH)_2D_3$. Thus, the absence of klotho results in increased serum levels of $1,25(OH)_2D_3$ and reduced serum concentrations of the calciotropic hormone parathyroid hormone.[4,7,8] This would drive increased resorption of Ca^{2+} from bone, hyperabsorption from the intestine, increased serum levels of Ca^{2+}, and consequently increase renal Ca^{2+} excretion. Definitive proof of this is lacking because the molecular control of Ca^{2+} homeostasis in klotho$^{-/-}$ mice has yet to be delineated.

Consistent with the above hypothesis is the observation that klotho$^{-/-}$ mice display hypercalciuria[4,5,9] and that normalization of serum $1,25(OH)_2D_3$ levels reverts many, but not all, of their abnormalities.[6] The published literature supports an alternative, complementary hypothesis.[9–11] A primary defect in tubular Ca^{2+} handling might cause hypervitaminosis D and renal Ca^{2+} wasting observed in klotho$^{-/-}$ mice. Consistent with this idea, *in vitro*, klotho mediates an increase in cell surface expression of transient receptor potential vanilloid 5 (TRPV5)[10,11] the distal convoluted tubule/connecting tubule (DCT/CNT) channel responsible for the transcellular absorption of Ca^{2+}.[12] This process is itself implicit to Ca^{2+} homeostasis as TRPV5 is the predominant regulator of urinary Ca^{2+} excretion.[13] Therefore, we set out to test the hypothesis that klotho$^{-/-}$ mice have a primary renal Ca^{2+} leak that contributes to a secondary increase in $1,25(OH)_2D_3$ synthesis and its consequences.

RESULTS

Klotho$^{-/-}$ Mice Show Hypercalcemia and Hypercalciuria

Klotho$^{-/-}$ mice between the age of 7 and 8 wk were housed for 24 h in metabolic cages, after which they were killed, serum was collected, and kidney, intestine, and bone were isolated. Klotho$^{-/-}$ mice display significant hypercalcemia and hyperphosphatemia (Figure 1A; Supplemental Tables 1 and 4). They are also significantly smaller than their wild-type littermates (Supplemental Table 2) and show increased renal Ca^{2+} excretion (Figure 1B). Klotho$^{-/-}$ mice have a lower urinary pH (Figure 1C), a reduced urine output, and more concentrated urine, although their daily water intake (when corrected for weight) is greater (Supplemental Table 2). The decrease in urinary volume remained significant even when urine output was corrected for the weight of the mice. To rule out the possibility that a metabolic acidosis was driving the aciduria, we performed venous blood gas analysis. The results indicated that klotho$^{-/-}$ mice had a respiratory acidosis (decreased plasma pH, increased CO_2, and increased bicarbonate; Supplemental Table 3).

Intestinal Hyperabsorption Contributes to Elevated Serum Ca^{2+} Levels in Klotho$^{-/-}$ Mice

We proceeded to evaluate the molecular mechanisms mediating active Ca^{2+} transport from the intestine. First, quantitative

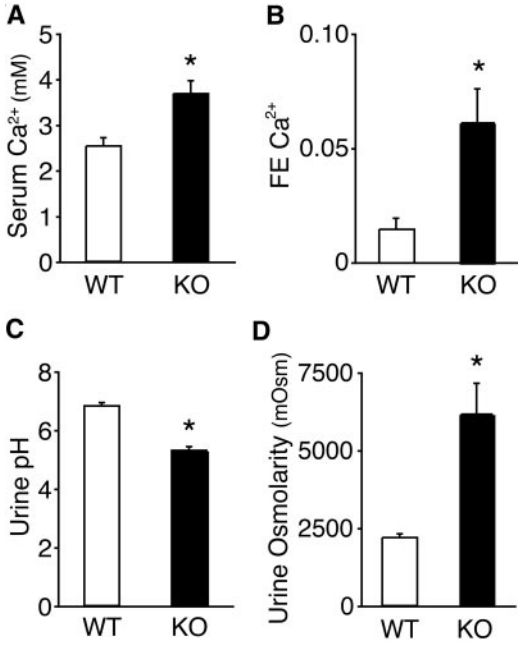

Figure 1. Klotho$^{-/-}$ mice characteristics. Plots of serum Ca^{2+} concentration (mM) (A), fractional excretion (FE) of Ca^{2+} (B), urine pH (C), and urine osmolarity (D) from wild-type and klotho$^{-/-}$ (KO) mice, $n = 10$ for both groups. $^*P < 0.05$ in comparison to wild-type.

real-time PCR (qPCR) was performed on duodenal samples from klotho$^{-/-}$ and wild-type mice for TRPV6, calbindin-D_{9K}, and plasma membrane Ca^{2+}-ATPase (PMCA1b). This showed an increase in the mRNA level of both TRPV6 and calbindin-D_{9K} in klotho$^{-/-}$ mice and no alteration in PMCA1b expression (Figure 2, A–C). These results are consistent with the elevated $1,25(OH)_2D_3$ levels present in klotho$^{-/-}$ mice (Supplemental Table 1). That the altered mRNA expression translated into increased protein expression was shown by immunoblotting for calbindin-D_{9K} (Figure 2, D and E). Importantly, the functional consequences of these observations were determined by measuring intestinal Ca^{2+} uptake. This showed that klotho$^{-/-}$ mice absorb $^{45}Ca^{2+}$ at a faster rate than their wild-type littermates (Figure 2F).

Opposite Expression Levels of Renal Ca^{2+} Transport Proteins in Klotho$^{-/-}$ Mice

The effect of increased intestinal Ca^{2+} uptake and $1,25(OH)_2D_3$ levels on the expression of renal Ca^{2+} handling proteins was assessed. First, using qPCR, the renal expression of TRPV5, calbindin-D_{28K}, NCX1, and PMCA1b was evaluated. The expression of TRPV5 mRNA was found to be significantly elevated (Figure 3A). In contrast, the expression of both NCX1 and calbindin-D_{28K} was decreased (Figure 3, B and C), whereas PMCA1b expression was unaltered (Figure 3D). We proceeded to substantiate these findings; first the protein expression of calbindin-D_{28K} was measured and determined to be downregulated via semiquantitative immunoblotting (Figure 3, E and F). Then, the level of TRPV5 protein expression was determined by quantification of

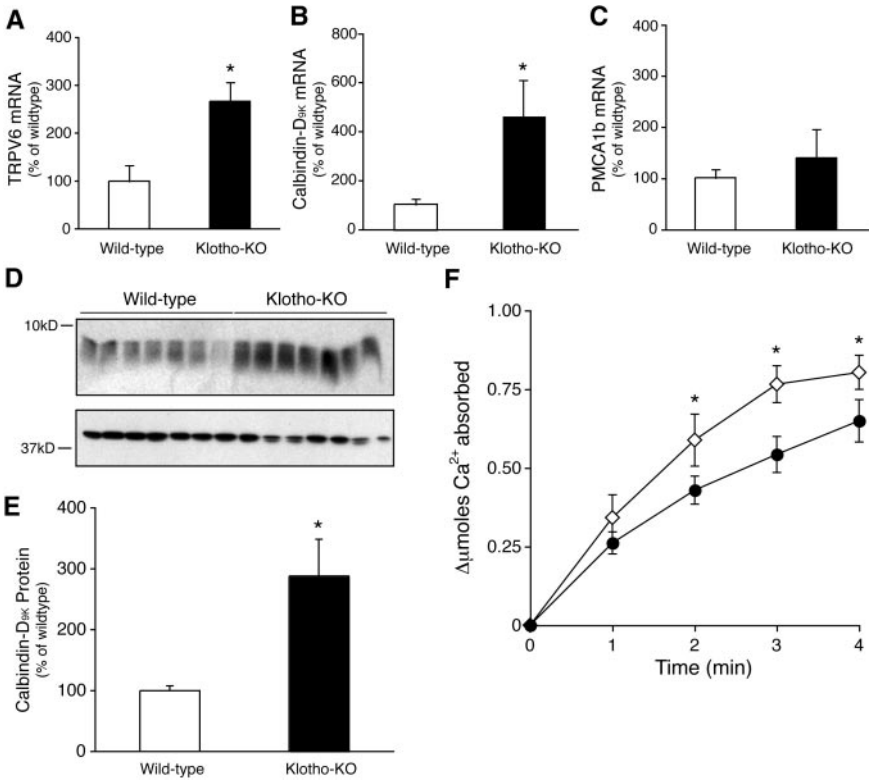

Figure 2. Characterization of intestinal Ca^{2+} handling. qPCR analysis of TRPV6 (A), calbindin-D_{9K} (B), and PMCA1b (C) expression in duodenum. The results are expressed as a percentage of wild-type and are normalized to the expression of HPRT, $n = 8$ per group. A representative immunoblot (D) and quantification (E) of calbindin-D_{9K} protein expression from wild-type and klotho$^{-/-}$ duodenum, $n = 7$ per group; note β-actin has been blotted (bottom panel) as a loading control. (F) $^{45}Ca^{2+}$ absorption into serum of wild-type (●) and klotho$^{-/-}$ (◇) mice after gastric gavage, $n = 8$ per group. *$P < 0.05$ in comparison to wild-type.

fluorescence from kidney sections that had been immunolabeled with an antibody against TRPV5. This was also in agreement with the findings of the mRNA analysis; TRPV5 protein expression was upregulated in the klotho$^{-/-}$ mice relative to their wild-type littermates (Figure 3, G and H).

To exclude the possibility of renal $1,25(OH)_2D_3$ resistance, we measured calbindin-D_{9K}, vitamin D receptor (VDR), and 25-hydroxyvitamin D-1-α-hydroxylase (1αOHase) mRNA expression in the kidney. Calbindin-D_{9K} expression was appropriately increased in the klotho$^{-/-}$ mice relative to their wild-type littermates on the control diet (Supplemental Figure 3A). The protein expression of calbindin-D_{9K} was upregulated in klotho$^{-/-}$ mice as well (Supplemental Figure 3D). VDR mRNA and protein expression was unaltered (Supplemental Figure 3, B and E), whereas 1αOHase was increased at the mRNA level in klotho$^{-/-}$ mice (Supplemental Figure 3C).

Klotho$^{-/-}$ Mice Develop Ca^{2+}-P(i) Precipitates in the DCT/CNT

The presence of concentrated urine and hypercalciuria prompted us to look at the expression of aquaporin-2. Semiquantitative immunoblot analysis of aquaporin-2 expression from kidney lysate of wild-type and klotho$^{-/-}$ mice showed an increased expression in klotho$^{-/-}$ mice (Figure 3, I and J), despite an elevated urinary Ca^{2+} excretion (Figure 1B). The functional consequence of hypercalciuria in klotho$^{-/-}$ mice was therefore studied.

Von Kossa staining identified Ca^{2+} precipitates throughout the cortex of the klotho$^{-/-}$ mice (Figure 4, A and B). Energy-dispersive x-ray microanalysis (EDX) measurements were used and showed that the precipitates consisted of Ca^{2+}-P(i) (Figure 4, E and F). Higher-resolution imaging was used to identify their location. Both electron microscopy and light microscopy of Toluidine blue–stained sections identified the presence of Ca^{2+}-P(i) precipitates decorating what appeared to be DCT/CNT (Figure 4, C and D). To confirm that the precipitates were predominately confined to the DCT/CNT, we performed von Kossa staining on knockout kidney sections and identified the DCT/CNT region by fluorescently labeling with calbindin-D_{28K} (Figure 4, G–I). This confirmed that many of the segments expressing calbindin-D_{28K} also contained precipitates (Figure 4, G-I; Supplemental Figure 1, A–C). To exclude the possibility that the precipitates were predominantly present in proximal tubules (PTs), after von Kossa staining, PTs were identified by immunofluorescent labeling with the breast cancer resistance protein.[14] This confirmed that the majority of Ca^{2+}-P(i) precipitates were not in the PT (Supplemental Figure 1, D–F). Renal pelvis dilation was not observed in klotho$^{-/-}$ mice, implying the absence of hydronephrosis or precipitates in the ureter.

Renal Ca^{2+} Wasting Is a Primary Defect in Klotho$^{-/-}$ Mice

To ascertain whether the renal Ca^{2+} leak was primary or secondary to an increased serum Ca^{2+} or $1,25(OH)_2D_3$ level, these parameters were normalized in the klotho$^{-/-}$ mice. This was accomplished by feeding the animals a low Ca^{2+}, P(i), and vitamin D ($<$0.13 μg/kg calciferol) diet (LVD) (Supplemental Tables 4 and 5). This diet increased the weight of the klotho$^{-/-}$ mice to that of the wild-type animals (Supplemental Table 5). LVD also brought the serum level of Ca^{2+} and $1,25(OH)_2D_3$ back into the normal range (Figure 5, A and B). Consistent with the hypothesis that klotho$^{-/-}$ mice have a primary renal Ca^{2+} leak, the normalization of these parameters failed to revert renal Ca^{2+} excretion to that of the wild-type animal (Figure 5C). Furthermore, the ex-

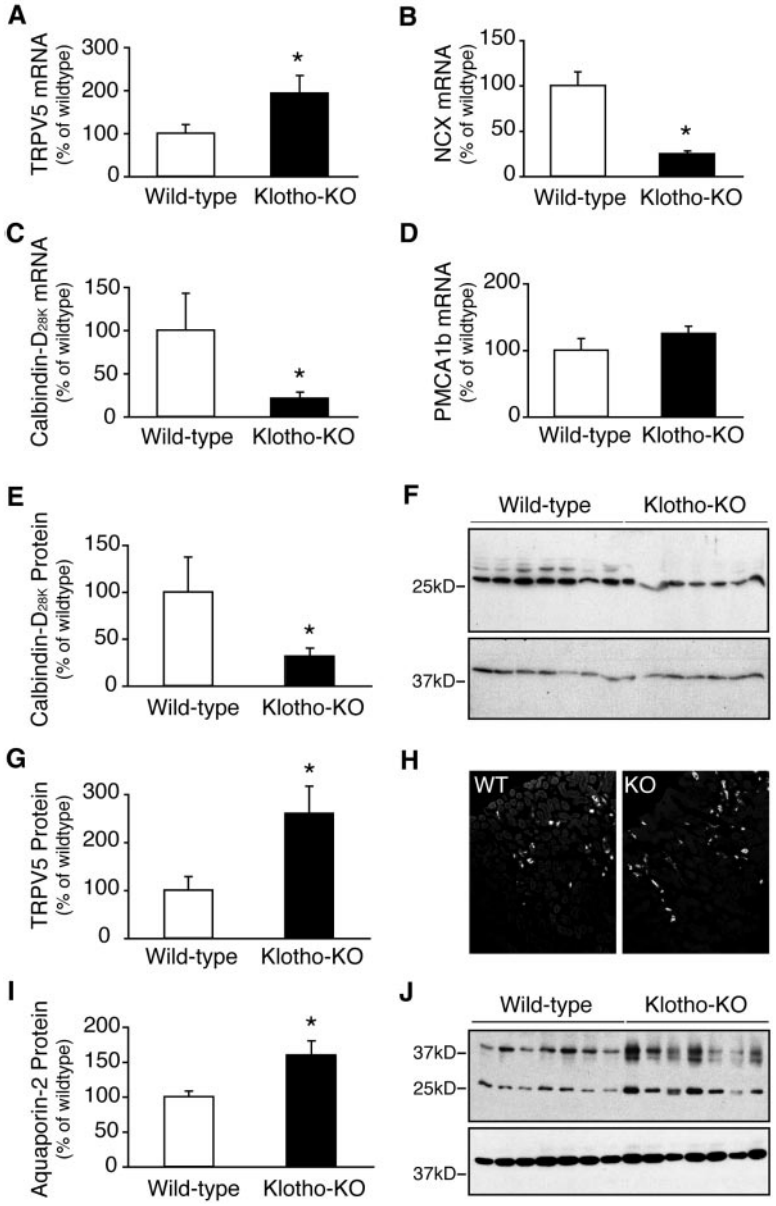

Figure 3. Characterization of the molecular mediators of renal transepithelial Ca^{2+} reabsorption. qPCR analysis of TRPV5 (A), NCX1 (B), calbindin-D_{28K} (C), and PMCA1b (D) mRNA expression in kidney. The results are expressed as a percentage of wild-type; both are normalized to the expression of HPRT, $n = 8$ per group. Representative immunoblot and quantification of calbindin-D_{28K} (E and F) and aquaporin-2 (I and J) protein expression from wild-type and klotho$^{-/-}$ (KO) whole kidney lysate, $n = 7$ per group. Note β-actin has been blotted (bottom panel) as a loading control. Quantification of TRPV5 protein expression in kidney of wild-type and klotho$^{-/-}$ (KO) mice (G), $n = 6$ per group. Representative images from the quantification are shown in H. *$P < 0.05$ in comparison to wild-type.

pression of TRPV5 remained elevated in klotho$^{-/-}$ mice, despite a greatly reduced $1,25(OH)_2D_3$ level, whereas calbindin-D_{28K} expression was consistently lower (Figure 5, D and E). However, intestinal and renal calbindin-D_{9K} expression returned to the level of the wild-type mice (Figure 5F; Supplemental Figure 3, A and D). Interestingly, renal cortical Ca^{2+} precipitates remained in some of the klotho$^{-/-}$ mice, albeit to a reduced extent, despite normalization of their serum Ca^{2+} and $1,25(OH)_2D_3$ levels (Supplemental Figure 2).

To assess the consequences on bone, a detailed structural analysis of femurs was performed. Klotho$^{-/-}$ mice have reduced bone mass compared with wild-type littermates (Figure 5G). Both trabecular and cortical thickness are significantly decreased, leading to lower trabecular and cortical bone volume and a severely reduced trabecular bone fraction (Figure 5G; Supplemental Table 6). Trabecular number is also significantly decreased in klotho$^{-/-}$ mice (Supplemental Table 6). On LVD, the bone phenotype of klotho$^{-/-}$ mice resembles that of wild-type mice fed the LVD diet (Figure 5G). This is corroborated by complete restoration of all bone structural parameters to wild-type values (Supplemental Table 6). In addition, LVD seems to increase femur length, perimeter, and femoral head volume in both wild-type and klotho$^{-/-}$ mice (Supplemental Table 6).

DISCUSSION

This study clearly showed that increased renal Ca^{2+} excretion in klotho$^{-/-}$ mice is a primary disturbance. It is neither the result of increased serum Ca^{2+} levels nor elevated $1,25(OH)_2D_3$ levels. Instead, our findings are consistent with a failure of klotho to maintain TRPV5 activity in the DCT/CNT (presumably through failing to retain it in the apical plasma membrane). Klotho$^{-/-}$ mice show hypercalcemia, elevated $1,25(OH)_2D_3$ levels, hyperabsorption of Ca^{2+} from their intestine, and severe osteopenia. Renal Ca^{2+} excretion is increased, despite elevated TRPV5 expression. However, the renal expression of calbindin-D_{28K} and NCX1 parallels that of the TRPV5 knockout mice; in both cases, they are reduced,[12,15] implying a failure for klotho$^{-/-}$ mice to reabsorb Ca^{2+} from the DCT/CNT via TRPV5. To exclude the possibility that renal Ca^{2+} wasting was secondary to increased serum Ca^{2+} or $1,25(OH)_2D_3$ levels, we normalized these parameters in the klotho$^{-/-}$ mice. This prevented the development of osteopenia and the increase in intestinal calbindin-D_{9K} expression. However, despite reduced serum Ca^{2+} and $1,25(OH)_2D_3$ levels, klotho$^{-/-}$ mice had persistently elevated renal Ca^{2+} excretion. Thus, renal Ca^{2+} wasting is a primary defect in klotho$^{-/-}$ mice. This in turn may in fact drive increased $1,25(OH)_2D_3$ synthesis, intestinal Ca^{2+} hyperabsorption, resorption from bone, and hypercalcemia.[16] Regardless, a primary renal Ca^{2+} leak contributes to nephrocalcinosis.

Central to the aging phenotype observed in klotho$^{-/-}$ mice

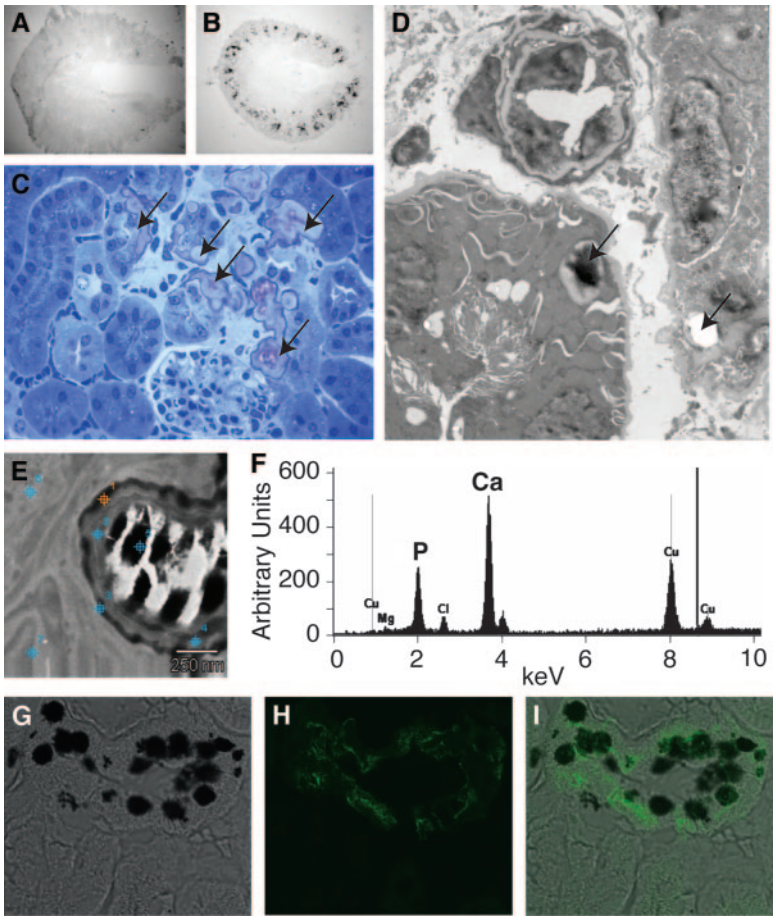

Figure 4. Klotho knockout mice show Ca^{2+}-phosphate precipitates. Low-power images of von Kossa–stained renal sections of wild-type (A) and klotho$^{-/-}$ (B) mice. Toluidine blue–stained renal section of a peri-glomerular, stone-containing region of a klotho$^{-/-}$ renal section (C); note arrows point to calcium precipitations. Transmission electron micrograph of renal cortex from a klotho$^{-/-}$ renal section (D); note arrows point to calcium precipitations. A representative energy map (E) and x-ray spectra (F) from EDX measurements performed on the Ca^{2+}-containing deposits. A high-magnification image of DCT/CNT (G–I) stained first with the von Kossa method to visualize Ca^{2+} and then immunostained with anti-calbindin-D_{28K} to localize the DCT/CNT.

is Ca^{2+} precipitation throughout many organ systems, not the least of which is the kidney as shown recently by Ohnishi et al.[8] This has been largely attributed to the formation of ectopic calcifications.[6] By examining the renal precipitations more closely, we were able to identify the presence of discrete calcifications confined to distinct tubular segments, suggesting a tubular pathology. The specific composition of the precipitates was delineated and found to be Ca^{2+}-P(i), a finding consistent with the increased renal Ca^{2+} and P(i) excretion observed in klotho$^{-/-}$ mice (Supplemental Table 2).[4,17] In fact, the dramatic increase in the urinary composition of these ions likely resulted in their precipitation. The exact location of the Ca^{2+}-P(i) precipitates was further studied, first with light and electron microscopy and then more specifically by immunofluorescence microscopy. Using the combination of von Kossa staining to detect Ca^{2+} deposits and nephron-specific immunofluorescence microscopy, we were able to localize the majority of precipitates to the DCT/CNT. This is the nephron segment where TRPV5[18] and klotho[17] are expressed. TRPV5 activity is required to absorb Ca^{2+} back into the blood from the DCT/CNT lumen.[12] It appears that a failure to do so, unless compensated by regulatory mechanisms, results in Ca^{2+}-P(i) precipitation. Although we observed cortical tubular precipitations or nephrocalcinosis, our results imply that within the ureter obstructions are not present nor do these mice suffer from hydronephrosis. Cases of obstructive nephropathy or hydronephrosis in either klotho$^{-/-}$ or FGF23$^{-/-}$ mice have not been reported in the literature. The acidification of urine provides a protective mechanism against Ca^{2+}-P(i) precipitation.[19] Klotho$^{-/-}$ mice have significantly acidified urine compared with their wild-type littermates. Their urinary acidification is not caused by a metabolic acidosis. Instead, it is likely a response to hypercalciuria and an attempt to prevent nephrocalcinosis. Thus, this finding provides further evidence of a renal Ca^{2+} leak. Another protective mechanism against nephrocalcinosis is urinary dilution. Increased delivery of Ca^{2+} to the DCT/CNT should dilute the urine by downregulating aquaporin-2 expression.[20] However, klotho$^{-/-}$ mice have concentrated urine compared with wild-type mice. This contributes to the formation of Ca^{2+}-P(i) precipitates and augments our understanding of this process. The reason for this apparent discrepancy is a greater need to protect intravascular volume than prevent stone formation. Klotho$^{-/-}$ mice would tend toward a reduced intravascular volume because they clearly have increased insensible losses. This latter phenomenon is the combined result of increased surface area to weight ratio and skin and lung disease. The presence of lung disease is evidenced by a respiratory acidosis in klotho$^{-/-}$ mice and the literature (Supplemental Table 3).[21,22] Regardless, clearly both acidification and dilution of urine are needed to prevent salt precipitations in the presence of increased Ca^{2+} excretion. A concentrated urine in the presence of hypercalciuria contributes to the formation of renal Ca^{2+}-P(i) precipitates in the klotho$^{-/-}$ mice.

Increased TRPV5 and decreased calbindin-D_{28K} and NCX1 expression is seemingly paradoxical. To exclude the possibility that they represent renal $1,25(OH)_2D_3$ resistance, we measured calbindin-D_{9K} and VDR expression (Supplemental Figure 3). Calbindin-D_{9K} expression was appropriately increased in the presence of increased $1,25(OH)_2D_3$ and reduced to wild-type levels by dietary restriction. Moreover, decreased VDR expression in klotho$^{-/-}$ mice cannot explain this observation. The observed upregulation of 1αOHase in klotho$^{-/-}$ mice is in agreement with the literature.[6,8] 1αOHase mRNA expression is also enhanced in FGF23$^{-/-}$ mice,[23] and administration of

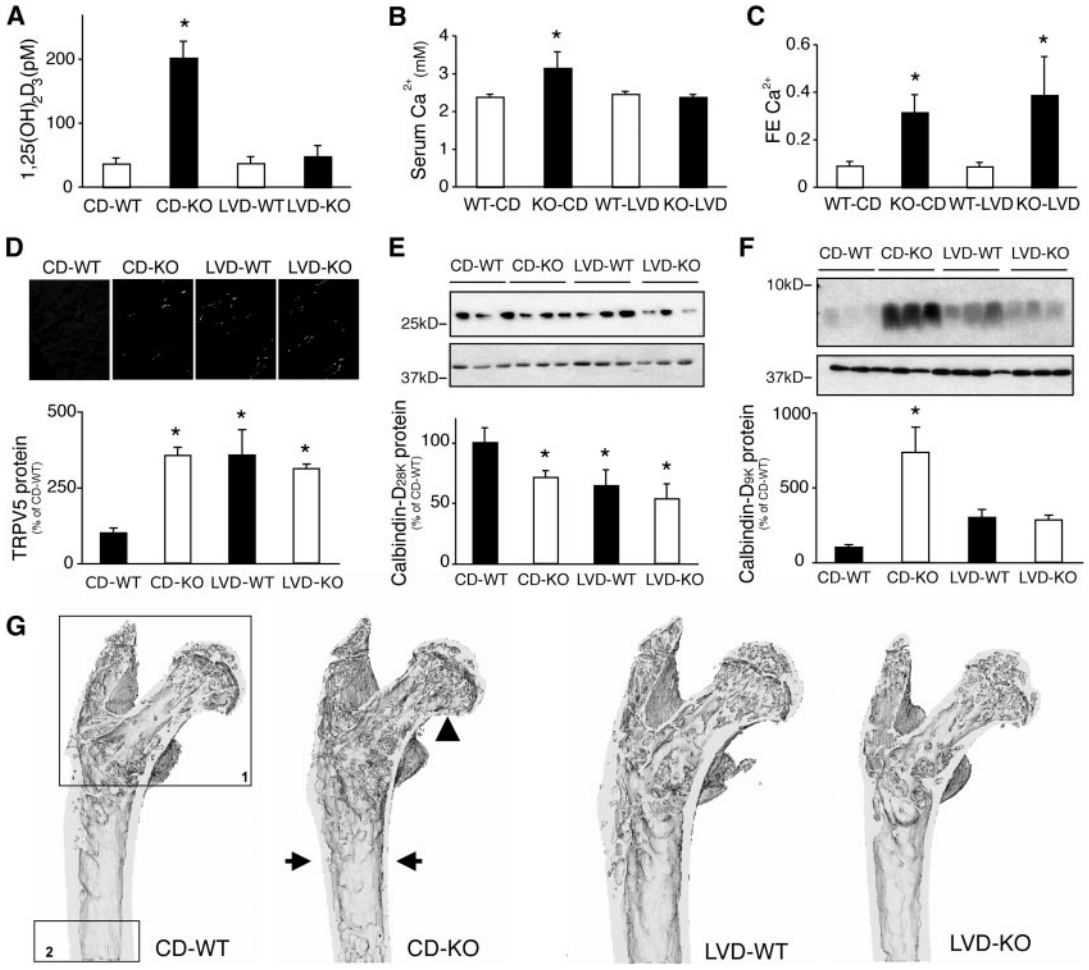

Figure 5. Characteristics of wild-type and klotho$^{-/-}$ mice on control diet and LVD. Serum levels of 1,25$(OH)_2D_3$ (A) and Ca^{2+} (B) from wild-type (WT) and klotho$^{-/-}$ (KO) mice on control diet (CD) or LVD, $n = 6$ per group. The fractional excretion (FE) of Ca^{2+} from wild-type and klotho$^{-/-}$ mice on either CD or LVD, $n = 6$ per group. Renal TRPV5 (D), calbindin-D_{28K} (E), or duodenal calbindin-D_{9K} (F) protein expression from wild-type and klotho$^{-/-}$ mice on either CD or LVD, $n = 6$ per group. (E and F) β-actin has been blotted as a loading control (bottom panel). (G) Representative three-dimensional reconstructions of femurs from wild-type and klotho$^{-/-}$ mice on either CD or LVD, $n = 4$ per group. Note the thinner cortices (arrows) and reduced trabecular bone volume (arrowhead) in the CD-KO mice. The black boxes indicate the scan areas for the analyses of (1) trabecular and (2) cortical bone, respectively. *$P < 0.05$ compared with CD-WT.

FGF23 to wildtype mice reduces *1αOHase* gene levels.[24] *In vitro* experiments have shown that the FGF23 signaling pathway is mediated via extracellular signal–regulated kinase 1/2.[24] These findings are consistent with klotho, in concert with FGF23, participating in an inhibitory feedback loop that results in the suppression of 1,25$(OH)_2D_3$ synthesis, as has also been discussed by others.[6] Regardless, rather than supporting the presence of renal 1,25$(OH)_2D_3$ resistance, these findings are compatible with a defect in active transcellular Ca^{2+} absorption from the DCT/CNT through TRPV5.[12,15] The rate of Ca^{2+} influx determines the level of calbindin-D_{28K} and NCX1 expression[12,15,25]; consequently, the low expression levels of these proteins suggest impaired Ca^{2+} influx through TRPV5. Although TRPV5 expression is increased, it is probably functionally insignificant, because TRPV5 is likely not retained in the plasma membrane because of the absence of klotho.[10,11] This is consistent with the observation that the application of klotho to cells expressing TRPV5 greatly increases cell surface expression and activity of the channel.[10,11] Specifically, *in vitro*, klotho, by cleaving the terminal sialic acid residue on the N-linked glycosylation site of TRPV5, exposes a glycosylation sequence that permits galectin-1 to retain TRPV5 in the apical membrane.[11] Moreover, microperfusion studies of isolated DCT/CNT from klotho$^{-/-}$ mice fail to show increased Ca^{2+} influx in the presence of parathyroid hormone,[9] a process mediated by TRPV5. Together these results provide strong evidence of a primary defect in DCT/CNT TRPV5 activation in klotho$^{-/-}$ mice, both *in vitro* and now *in vivo*. Our findings support a central role for klotho in Ca^{2+} homeostasis by preventing renal Ca^{2+} loss and the commonly associated problems nephrolithiasis and osteopenia. Both of these clinical problems occur more frequently with advanced age, as does

the incidence of hypercalciuria. Thus, our results provide further molecular details of the contribution of klotho to the problems associated with advanced age.

To exclude the possibility that the increased Ca^{2+} excretion observed in klotho$^{-/-}$ mice was caused by a secondary effect of hypervitaminosis D or hypercalcemia, we normalized both these parameters. This experiment clearly showed that the fractional excretion of Ca^{2+} in klotho$^{-/-}$ mice remains elevated, even in the absence of increased serum $1,25(OH)_2D_3$ or Ca^{2+} levels. In contrast, the elevated levels of calbindin-D_{9K} were normalized by this perturbation, suggesting that elevated $1,25(OH)_2D_3$ levels were driving their expression. This result is similar to that observed in bone. Normalization of serum $1,25(OH)_2D_3$ levels in klotho$^{-/-}$ mice prevented osteopenia, suggesting that this abnormality may also be secondary to the increased $1,25(OH)_2D_3$ level. Although renal Ca^{2+} wasting will cause increased serum $1,25(OH)_2D_3$ levels, we cannot exclude the role of klotho in FGF23 signaling from contributing to this abnormality in klotho$^{-/-}$ mice. Indeed both these mechanisms likely contribute to the particularly elevated levels of serum $1,25(OH)_2D_3$ and Ca^{2+} observed in these animals.

Our results clearly showed a reduction in cortical volume, trabecular density, and trabeculae number in klotho$^{-/-}$ mice on a control diet (Supplemental Table 6). Consequently, the thinner trabecular bone structures become apparent in the 3D reconstruction (Figure 5G). Our observations differ from the previously reported studies[26–31] in that we found decreased trabecular thickness, volume, and number per area; however, our cortical analyses are consistent with these reports. The trabecular differences may be because of the age of the mice we analyzed (7 to 8 wk old *versus* 4 to 5 wk in some studies[28–30]). Perhaps in these weeks, accelerated aging occurs, which could explain the observed discrepancy. Another variation between some of those reports and ours is the long bone studied. We performed detailed analysis on femurs, whereas previous authors have focused more on the tibia.[26,30] The genetic background of the klotho$^{-/-}$ mice also differs between some of these reports. In our experiments, klotho$^{-/-}$ mice with a C57Bl6 background were used, whereas Yamashita *et al.*[31] performed studies in klotho$^{-/-}$ mice generated from a C3H strain. Furthermore, as with the other studies, ours was completed on young mice with immature skeletons; as such, these results may not apply to an aging skeleton.

In summary, we provide *in vivo* data consistent with decreased TRPV5 activity in klotho$^{-/-}$ mice. This is a primary consequence of the absence of klotho and not secondary to elevated serum Ca^{2+} and $1,25[OH)]_2D_3$ levels. In fact, these latter findings are likely a direct consequence of this abnormality, because the expression of Ca^{2+}-transporting proteins was normalized and osteopenia was prevented by reducing the serum concentration of $1,25(OH)_2D_3$. In contrast, this fails to return the fractional excretion of Ca^{2+} to that of the wild-type animals, providing direct evidence for a primary renal Ca^{2+} leak. This likely drives the hypervitaminosis D and hypercalciuria and contributes to the formation of nephrocalcinosis in DCT/CNT of klotho$^{-/-}$ mice. We therefore provided evidence that klotho activates TRPV5 *in vivo*, thereby explaining its central role in Ca^{2+} homeostasis.

CONCISE METHODS

Generation and Characterization of Klotho$^{-/-}$ Mice

Heterozygous klotho$^{-/-}$ mice were purchased from Mutant Mouse Regionale Resource Centers (ID: 011732-UCD); the details of their generation are provided elsewhere.[32] These were bred to C57Bl/6 wild-type animals, and the heterozygous offspring were crossed to produce klotho$^{-/-}$ animals. Standard pelleted chow (0.25% [wt/vol] Na, 1.1% [wt/vol] Ca, 0.2% [wt/vol] Mg, 0.7% [wt/vol] P(i), and 0.9% [wt/vol] K) and drinking water were available *ad libitum*. Klotho$^{-/-}$ and wild-type animals were housed in metabolic cages for 24 h at a time ($n = 10$ of each). All experiments were performed in compliance with the animal ethics board of the Radboud University Nijmegen.

Low Ca^{2+}, P(i), and $1,25(OH)_2D_3$ Diet

After crossing heterozygous pairs, produced as described above, pregnant females were separated into individual cages and allocated to either the control diet (CD) or LVD. The content of the control, synthetic diet consisted of {0.19% [wt/vol] Na, 0.9% [wt/vol] Ca, 0.21% [wt/vol] Mg, 0.63% [wt/vol] P, and 0.97% [wt/vol] K, and 1500 IU $1,25(OH)_2D_3$}, and the LVD contained (0.19% [wt/vol] Na, 0.34% [wt/vol] Ca, 0.21% [wt/vol] Mg, 0.22% [wt/vol] P, 0.97% [wt/vol] K, and <5 IU Vitamin D). Lactating mothers continued to receive the allocated diet, and the pups, on weaning, were fed the appropriate diet. Between 7 and 8 wk of age, the klotho$^{-/-}$ mice and wild-type animals were housed in metabolic cages for 24 h, after which blood was collected, mice were killed, and tissue was sampled.

Characterization of Ca^{2+} Homeostasis

Serum and urine Ca^{2+} concentration was determined using a colorimetric assay kit as described previously.[33] A flame spectrophotometer (FCM 6343; Eppendorf, Hamburg, Germany) was used to measure serum and urine Na^+ concentrations and urine K^+ concentrations. Serum and urine P(i) and creatinine concentrations and venous blood gases were determined using a Hitachi autoanalyzer (Hitachi, Laval, Quebec, Canada). Serum and urine osmolarity was obtained using a Halbmikro-Osmometer K-7400 (Knauer, Berlin, Germany). The *in vivo* $^{45}Ca^{2+}$ absorption assay was performed as described elsewhere.[34] qPCR for TRPV5, TRPV6, calbindin-D_{9K}, calbindin-D_{28K}, NCX1, PMCA1b, VDR, and 1αOHase was completed essentially as described previously.[35–37] Immunohistochemistry and its quantification for TRPV5 followed the procedure detailed elsewhere.[38] Semiquantitative immunoblotting for calbindin-D_{28K}, calbindin-D_{9K}, and aquaporin-2 has been described previously[39,40] Polyclonal anti-VDR antibody (Santa Cruz Biotechnology, Santa Cruz, CA) was used at a dilution of 1:200. Von Kossa staining was performed to visualize Ca^{2+}-containing precipitates.

Electron Microscopy

Renal tubular Ca^{2+} precipitations were analyzed by transmission electron microscopy. Kidney samples were fixed in 2.5% (wt/vol) glutaraldehyde dissolved in 0.1 M cacodylate buffer, pH 7.4, at room temperature for 2 h after dissection. Samples were subsequently washed three times with 0.1 M sodium cacodylate buffer and postfixed with 1% (wt/vol) osmium tetroxide in 0.1 M sodium cacodylate buffer at room temperature for 1 h. Samples were dehydrated and processed for embedding in Epon resin. Polymerization was performed in a 60°C oven. For morphology studies, sections were cut using a diamond knife and mounted on copper grids (100 mesh). Sections were stained with uranyl acetate and lead citrate and examined using a Jeol 1200 EX II. For EDX measurements, section thickness was approximately 200 nm, and postfixation was omitted, not contrasted, and subsequently examined using a Jeol 1200/STEM in combination with a Thermo Noran microanalysis SIX system (Thermo Fisher Scientific, Waltham, MA). Accelerated voltage of 60 keV was used for x-ray microanalysis. X-ray spectra and maps for Ca^{2+} and P(i) distribution were acquired.

Bone Structural Analysis

After fixation in 10% (wt/vol) formalin and measuring their lengths, femurs from both wildtype and klotho$^{-/-}$ mice on control diet (CD-WT and CD-KO, respectively; $n = 4$) and wildtype and klotho$^{-/-}$ mice on LVD (LVD-WT and LVD-KO, respectively; $n = 4$) were studied in detail by scanning them in an *in vivo* microcomputed tomography scanner (Skyscan 1076; Skyscan, Aartselaar, Belgium). Scans were processed, and three-dimensional morphometric analyses of the bones were performed, using free software of the 3D-calculator project (www.skyscan.be/products/downloads.htm) as described earlier.[12] All parameters were expressed according to the bone histomorphometry nomenclature.[41] The region of interest was confined to the proximal half of the femur and contained both trabecular (scan area, 0 to 4.1 mm; indicated in Figure 5G) and cortical (scan area, 7.2 to 8.1 mm) bone structures, enabling accurate analysis of a number of parameters in both compartments. Using several software packages, three-dimensional representations were made from femurs of each experimental group.

Statistical Analysis

Data are expressed as mean ± SEM. Statistical comparisons were analyzed by one-way ANOVA with a Bonferroni correction for multiple comparison. A $P < 0.05$ was considered statistically significant. All analyses were performed using the SPSS Statistical Package software (Power PC version 4.51; Abacus Concepts).

Further details of the materials and methods can be found online.

ACKNOWLEDGMENTS

R.T.A. is supported by a phase I Clinician Scientist award from the Canadian Institute of Health Research and a KRESCENT postdoctoral award from the Kidney Foundation of Canada. This work was supported by The Netherlands Organization for Scientific Research (NWO-ALW 814.02.001, NWO-CW 700.55.302, ZonMw 9120.6110), EURYI award from the European Science Foundation, and the Dutch Kidney foundation (C03.6017, C06.2170). We thank Henk Arnts and Bianca Lemmers-Van de Weem (CDL, UMC Nijmegen) for their excellent technical assistance with the animal experiments and Sander Botter of the Erasmus MC, Rotterdam, The Netherlands, for his technical assistance concerning the microcomputed tomography procedures.

DISCLOSURES

None.

REFERENCES

1. Kuro-o M, Matsumura Y, Aizawa H, Kawaguchi H, Suga T, Utsugi T, Ohyama Y, Kurabayashi M, Kaname T, Kume E, Iwasaki H, Iida A, Shiraki-Iida T, Nishikawa S, Nagai R, Nabeshima YI: Mutation of the mouse klotho gene leads to a syndrome resembling ageing. *Nature* 390: 45–51, 1997
2. Kuro-o M: Klotho as a regulator of fibroblast growth factor signaling and phosphate/calcium metabolism. *Curr Opin Nephrol Hypertens,* 15: 437–441, 2006
3. Torres PU, Prie D, Molina-Bletry V, Beck L, Silve C, Friedlander G: Klotho: An antiaging protein involved in mineral and vitamin D metabolism. *Kidney Int,* 71: 730–737, 2007
4. Yahata K, Mori K, Mukoyama M, Sugawara A, Suganami T, Makino H, Nagae T, Fujinaga Y, Nabeshima Y, Nakao K: Regulation of stanniocalcin 1 and 2 expression in the kidney by klotho gene. *Biochem Biophys Res Commun* 310: 128–134, 2003
5. Segawa H, Yamanaka S, Ohno Y, Onitsuka A, Shiozawa K, Aranami F, Furutani J, Tomoe Y, Ito M, Kuwahata M, Imura A, Nabeshima Y, Miyamoto K: Correlation between hyperphosphatemia and type II Na-Pi cotransporter activity in klotho mice. *Am J Physiol Renal Physiol* 292: F769–F779, 2007
6. Tsujikawa H, Kurotaki Y, Fujimori T, Fukuda K, Nabeshima Y: Klotho, a gene related to a syndrome resembling human premature aging, functions in a negative regulatory circuit of vitamin D endocrine system. *Mol Endocrinol* 17: 2393–2403, 2003
7. Yoshida T, Fujimori T, Nabeshima Y: Mediation of unusually high concentrations of 1,25-dihydroxyvitamin D in homozygous klotho mutant mice by increased expression of renal 1alpha-hydroxylase gene. *Endocrinology* 143: 683–689, 2002
8. Ohnishi M, Nakatani T, Lanske B, Razzaque MS: Reversal of mineral ion homeostasis and soft-tissue calcification of klotho knockout mice by deletion of vitamin D 1alpha-hydroxylase. *Kidney Int* 75: 1166–1172, 2009
9. Tsuruoka S, Nishiki K, Ioka T, Ando H, Saito Y, Kurabayashi M, Nagai R, Fujimura A: Defect in parathyroid-hormone-induced luminal calcium absorption in connecting tubules of Klotho mice. *Nephrol Dial Transplant* 21: 2762–2767, 2006
10. Chang Q, Hoefs S, van der Kemp AW, Topala CN, Bindels RJ, Hoenderop JG: The beta-glucuronidase klotho hydrolyzes and activates the TRPV5 channel. *Science* 310: 490–493, 2005
11. Cha SK, Ortega B, Kurosu H, Rosenblatt KP, Kuro-o M, Huang CL: Removal of sialic acid involving Klotho causes cell-surface retention of TRPV5 channel via binding to galectin-1. *Proc Natl Acad Sci U S A* 105: 9805–9810, 2008
12. Hoenderop JG, van Leeuwen JP, van der Eerden BC, Kersten FF, van der Kemp AW, Merillat AM, Waarsing JH, Rossier BC, Vallon V, Hummler E, Bindels RJ: Renal Ca^{2+} wasting, hyperabsorption, and reduced bone thickness in mice lacking TRPV5. *J Clin Invest* 112: 1906–1914, 2003

13. Mensenkamp AR, Hoenderop JG, Bindels RJ: TRPV5, the gateway to Ca^{2+} homeostasis. *Handb Exp Pharmacol* 179: 207–220, 2007
14. Huls M, Brown CD, Windass AS, Sayer R, van den Heuvel JJ, Heemskerk S, Russel FG, Masereeuw R: The breast cancer resistance protein transporter ABCG2 is expressed in the human kidney proximal tubule apical membrane. *Kidney Int* 73: 220–225, 2008
15. Renkema KY, Nijenhuis T, van der Eerden BC, van der Kemp AW, Weinans H, van Leeuwen JP, Bindels RJ, Hoenderop JG: Hypervitaminosis D mediates compensatory Ca^{2+} hyperabsorption in TRPV5 knockout mice. *J Am Soc Nephrol* 16: 3188–3195, 2005
16. Selby PL, Davies M, Marks JS, Mawer EB: Vitamin D intoxication causes hypercalcaemia by increased bone resorption which responds to pamidronate. *Clin Endocrinol (Oxf)* 43: 531–536, 1995
17. Li SA, Watanabe M, Yamada H, Nagai A, Kinuta M, Takei K: Immunohistochemical localization of Klotho protein in brain, kidney, and reproductive organs of mice. *Cell Struct Funct* 29: 91–99, 2004
18. Loffing J, Loffing-Cueni D, Valderrabano V, Klausli L, Hebert SC, Rossier BC, Hoenderop JG, Bindels RJ, Kaissling B: Distribution of transcellular calcium and sodium transport pathways along mouse distal nephron. *Am J Physiol Renal Physiol* 281: F1021–F1027, 2001
19. Wagner CA: When proton pumps go sour: Urinary acidification and kidney stones. *Kidney Int* 73: 1103–1105, 2008
20. Earm JH, Christensen BM, Frokiaer J, Marples D, Han JS, Knepper MA, Nielsen S: Decreased aquaporin-2 expression and apical plasma membrane delivery in kidney collecting ducts of polyuric hypercalcemic rats. *J Am Soc Nephrol* 9: 2181–2193, 1998
21. Sato A, Hirai T, Imura A, Kita N, Iwano A, Muro S, Nabeshima Y, Suki B, Mishima M: Morphological mechanism of the development of pulmonary emphysema in klotho mice. *Proc Natl Acad Sci U S A* 104: 2361–2365, 2007
22. Suga T, Kurabayashi M, Sando Y, Ohyama Y, Maeno T, Maeno Y, Aizawa H, Matsumura Y, Kuwaki T, Kuro OM, Nabeshima Y, Nagai R: Disruption of the klotho gene causes pulmonary emphysema in mice. Defect in maintenance of pulmonary integrity during postnatal life. *Am J Respir Cell Mol Biol* 22: 26–33, 2000
23. Nakatani T, Sarraj B, Ohnishi M, Densmore MJ, Taguchi T, Goetz R, Mohammadi M, Lanske B, Razzaque MS: In vivo genetic evidence for klotho-dependent, fibroblast growth factor 23 (Fgf23) -mediated regulation of systemic phosphate homeostasis. *Faseb J* 23: 433–441, 2009
24. Perwad F, Zhang MY, Tenenhouse HS, Portale AA: Fibroblast growth factor 23 impairs phosphorus and vitamin D metabolism in vivo and suppresses 25-hydroxyvitamin D-1alpha-hydroxylase expression in vitro. *Am J Physiol Renal Physiol* 293: F1577–F1583, 2007
25. Nijenhuis T, Vallon V, van der Kemp AW, Loffing J, Hoenderop JG, Bindels RJ: Enhanced passive Ca2+ reabsorption and reduced Mg^{2+} channel abundance explains thiazide-induced hypocalciuria and hypomagnesemia. *J Clin Invest* 115: 1651–1658, 2005
26. Kawaguchi H, Manabe N, Miyaura C, Chikuda H, Nakamura K, Kuro-o M: Independent impairment of osteoblast and osteoclast differentiation in klotho mouse exhibiting low-turnover osteopenia. *J Clin Invest* 104: 229–237, 1999
27. Kawaguchi H, Manabe N, Chikuda H, Nakamura K, Kuroo M: Cellular and molecular mechanism of low-turnover osteopenia in the klotho-deficient mouse. *Cell Mol Life Sci* 57: 731–737, 2000
28. Suzuki H, Amizuka N, Oda K, Noda M, Ohshima H, Maeda T: Histological and elemental analyses of impaired bone mineralization in klotho-deficient mice. *J Anat* 212: 275–285, 2008
29. Yamashita T, Nabeshima Y, Noda M: High-resolution micro-computed tomography analyses of the abnormal trabecular bone structures in klotho gene mutant mice. *J Endocrinol* 164: 239–245, 2000
30. Kashimada K, Yamashita T, Tsuji K, Nifuji A, Mizutani S, Nabeshima Y, Noda M: Defects in growth and bone metabolism in klotho mutant mice are resistant to GH treatment. *J Endocrinol* 174: 403–410, 2002
31. Yamashita T, Okada S, Higashio K, Nabeshima Y, Noda M: Double mutations in klotho and osteoprotegerin gene loci rescued osteopetrotic phenotype. *Endocrinology* 143: 4711–4717, 2002
32. Takeshita K, Fujimori T, Kurotaki Y, Honjo H, Tsujikawa H, Yasui K, Lee JK, Kamiya K, Kitaichi K, Yamamoto K, Ito M, Kondo T, Iino S, Inden Y, Hirai M, Murohara T, Kodama I, Nabeshima Y: Sinoatrial node dysfunction and early unexpected death of mice with a defect of klotho gene expression. *Circulation* 109: 1776–1782, 2004
33. Bindels RJ, Hartog A, Abrahamse SL, Van Os CH: Effects of pH on apical calcium entry and active calcium transport in rabbit cortical collecting system. *Am J Physiol* 266: F620–F627, 1994
34. Van Cromphaut SJ, Dewerchin M, Hoenderop JG, Stockmans I, Van Herck E, Kato S, Bindels RJ, Collen D, Carmeliet P, Bouillon R, Carmeliet G: Duodenal calcium absorption in vitamin D receptor-knockout mice: functional and molecular aspects. *Proc Natl Acad Sci U S A* 98: 13324–13329, 2001
35. Nijenhuis T, Hoenderop JG, Loffing J, van der Kemp AW, van Os CH, Bindels RJ: Thiazide-induced hypocalciuria is accompanied by a decreased expression of Ca^{2+} transport proteins in kidney. *Kidney Int* 64: 555–564, 2003
36. van Abel M, Huybers S, Hoenderop JG, van der Kemp AW, van Leeuwen JP, Bindels RJ: Age-dependent alterations in Ca^{2+} homeostasis: role of TRPV5 and TRPV6. *Am J Physiol Renal Physiol* 291: F1177–F1183, 2006
37. van Abel M, Hoenderop JG, van der Kemp AW, van Leeuwen JP, Bindels RJ: Regulation of the epithelial Ca^{2+} channels in small intestine as studied by quantitative mRNA detection. *Am J Physiol Gastrointest Liver Physiol* 285: G78–G85, 2003
38. Hoenderop JG, Hartog A, Stuiver M, Doucet A, Willems PH, Bindels RJ: Localization of the epithelial Ca^{2+} channel in rabbit kidney and intestine. *J Am Soc Nephrol* 11: 1171–1178, 2000
39. Huybers S, Apostolaki M, van der Eerden BC, Kollias G, Naber TH, Bindels RJ, Hoenderop JG: Murine TNF(DeltaARE) Crohn's disease model displays diminished expression of intestinal Ca^{2+} transporters. *Inflamm Bowel Dis* 14: 803–811, 2008
40. Kamsteeg EJ, Heijnen I, van Os CH, Deen PM: The subcellular localization of an aquaporin-2 tetramer depends on the stoichiometry of phosphorylated and nonphosphorylated monomers. *J Cell Biol* 151: 919–930, 2000
41. Parfitt AM, Simon LS, Villanueva AR, Krane SM: Procollagen type I carboxy-terminal extension peptide in serum as a marker of collagen biosynthesis in bone. Correlation with Iliac bone formation rates and comparison with total alkaline phosphatase. *J Bone Miner Res* 2: 427–436, 1987

Supplemental information for this article is available online at http://www.jasn.org/.